Italian Association of Aeronautics and Astronautics
XXV International Congress
9-12 September 2019 | Rome, Italy

A QUASI-LINEAR PARAMETER VRYING (QLPV) MODELING APPROACH FOR TILTROTOR CONVERSION MANOEUVRE

H. N. Nabi[1, 2*], G. Quaranta[1]

[1]Department of Aerospace Science and Technology, Politecnico di Milano, Milan, Italy

[2]Department of Control and Operations, Faculty of Aerospace Engineering, Delft University of Technology, Delft, The Netherlands

* hafiznoor.nabi@polimi.it, h.n.nabi@tudelft.nl

ABSTRACT

A high order quasi-Linear Parameter Varying model is developed for XV-15 that combines discrete state-space models to provide a continuous model dynamics and trim characteristics during the conversion manoeuvre. Tracking control system based on gain scheduled linear quadratic tracker with integrator (LQTI) is designed in order to perform automatic conversion manoeuvre for XV-15 based on the qLPV model.

Keywords: Tiltrotor, conversion manoeuvre, qLPV, LQTI

1 INTRODUCTION

Tiltrotors can operate over a broad flight envelope. They have the ability to hover like a helicopter and fly at relatively high cruise speeds and range like a fixed wing airplane. There are a lot of technical challenges associated with designing a tiltrotor aircraft to enable their extensive flight envelope and to perform satisfactorily over a broad range of flight configurations.

Tiltrotor performs a conversion manoeuvre to transform from a helicopter mode to an airplane mode and vice versa. A safe conversion is performed within a constrained region in the airspeed versus nacelle angle graph, called the conversion corridor, shown in Figure 1 for the case of XV-15. Currently, the conversion manoeuvre is flown by the pilot and in general the pilot workload is higher than in other phases of flight. This situation may not be optimal in particular, considering the possibility to perform conversion manoeuvre in a civil tiltrotor aircraft while being guided by the Air Traffic Control (ATC). Moreover, conversion from helicopter to airplane configuration and vice versa is characterized by high structural loads, both on rotor and airframe [1, 2].

In order to ensure safety by reducing pilot workload and limit the loads during the conversion manoeuvre, an automatic conversion system is required. Such systems are envisioned in the patents [4, 5]. An optimal conversion manoeuvre trajectory can be predetermined based on safe length from upper and lower boundaries of the conversion corridor, minimizing aeroelastic instabilities and structural loads etc. This optimal conversion manoeuvre is then either displayed to the pilot in order to assist in manual conversion and/or automatically performed by Flight Control System (FCS). An initial work on optimization of tiltrotor conversion manoeuvre is presented in Righetti et al. [6].

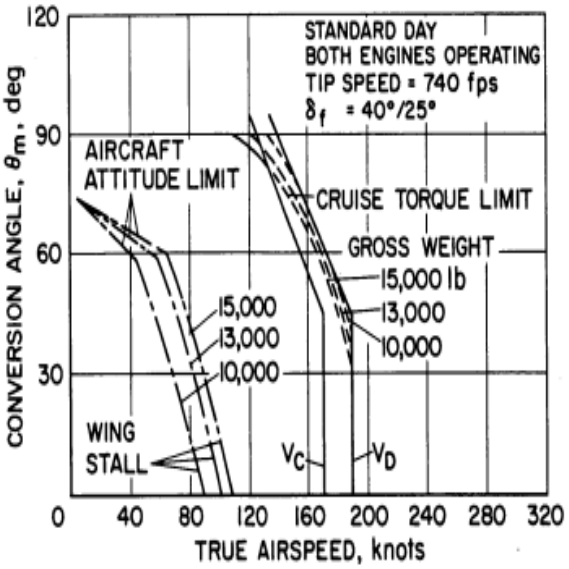

Figure 1: XV-15 conversion corridor [3]

In the current study, a quasi-Linear Parameter Varying (qLPV) or model stitching technique [7, 8] is employed for modelling the flight dynamics of a tiltrotor in the conversion corridor. In this technique, the aerodynamic stability and control derivatives and trim data at each discrete equilibrium point are stored in lookup tables as function of scheduling parameters. The corresponding trim data and derivatives are combined with nonlinear equations of motion and nonlinear gravitational force equations to obtain a continuous qLPV "stitched" model. A low order qLPV model for NASA's LCTR2 (Large Civil Tiltrotor, 2nd generation) was developed in [9] for the purpose of handling quality analyses in hover and low speed. Most recently, qLPV models for a coaxial-pusher helicopter and a tiltrotor aircraft were developed by Berger et al. [10]. In both studies, linear state-space models were scheduled with two parameters only: velocity V and nacelle angle β_i. However, in the current research models are scheduled with four parameters: altitude h, nacelle angle β_i, wing flap angle δ_f and veclocity V.

The paper is organized as follows: development of qLPV model is described in detail in section 2. In section 3, control synthesis of LQTI controller and results of an automatic conversion manoeuvre are presented. Lastly, a brief conclusion is presented in section 4.

2 QUASI-LINEAR PARAMETER VARYING (QLPV) MODEL

2.1 Theory

Linear Parameter Varying (LPV) models are linear state-space models that depend on time varying scheduling parameters $\rho(t)$. In this approach, linear state-space models obtained at discrete trim points are interpolated through lookup tables as function of scheduling parameters. The LPV model is defined as [7]:

$$\dot{\mathbf{x}}(t) = A\big(\rho(t)\big)\mathbf{x}(t) + B\big(\rho(t)\big)\mathbf{u}(t) \tag{1}$$

A particular case of LPV model is when subset of scheduling parameters is also state of the system, such models are called quasi-LPV. If the state vector $\mathbf{x}(t)$ can be decomposed into scheduling states $\mathbf{z}(t)$ and non-scheduling states $\mathbf{w}(t)$, then the qLPV model is defined as:

$$\begin{bmatrix}\dot{\mathbf{z}}(t)\\ \dot{\mathbf{w}}(t)\end{bmatrix} = A\big(\rho(t)\big)\begin{bmatrix}\mathbf{z}(t)\\ \mathbf{w}(t)\end{bmatrix} + B\big(\rho(t)\big)\mathbf{u}(t) \tag{2}$$

An extension to the qLPV model is the stitched model [8], where LPV model is combined with nonlinear equations of motion including nonlinear gravitational forces.

2.2 Linear Models

In order to develop a continuous LPV model, discrete aeroelastic linear models of XV-15 are obtained using MASST (Modern Aeroservoelastic State Space Tools), developed at Politecnico di Milano [11, 12]. Rotor aeroelastic models in MASST are obtained from CAMRAD/JA [13] using data published in [14, 15].

Linear state-space models and corresponding trim data are obtained throughout the conversion corridor. Furthermore, models are obtained at four wing flap δ_f settings ($\delta_f = [0\ 20\ 40\ 75]$ deg.) and at two altitudes ($h = [0\ 10000]$ ft). The grid of linear state-space models for a particular wing flap angle and altitude is shown in Figure 2. Rectangular regular grid is generated by clipping and keeping the edge models.

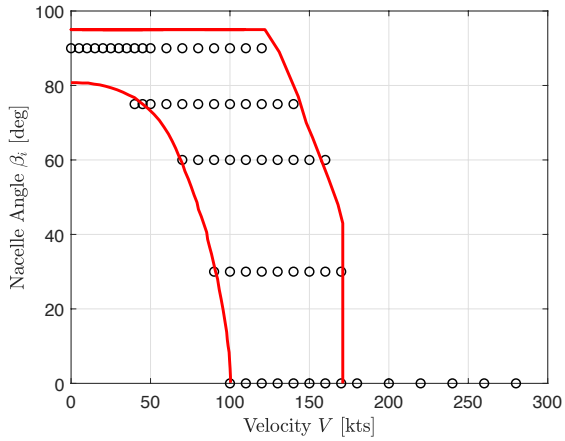

Figure 2: XV-15 linear state-space models and conversion corridor

The linear state-space models obtained through MASST contain 85 states including rigid body states (9), wing bending 1st mode (2), three blade bending modes in multi-blade coordinates for each rotor (36), two blade torsional modes in multi-blade coordinates for each rotor (24), two gimbal states for each rotor (8) and three inflow states for each rotor based on the Pit Peters model [16] (6). And 10 inputs including 6 rotor controls (collective pitch θ_0, longitudinal θ_{1s} and lateral θ_{1c} cyclic for each rotor) and 4 aerodynamic control surface deflections (wing flap δ_f, elevator δ_e, rudder δ_r and aileron δ_a).

2.3 qLPV Model

Linear state-space models are scheduled with $\rho(t) = [h\ \ \beta_i\ \ \delta_f\ \ V]$ to obtain a continuous qLPV model, shown in Figure 3. Two of the scheduling parameters, velocity V and altitude h, are dependent upon the states of linear system and hence making the system quasi-LPV. This state dependency may cause nonlinear feedback.

Trim states, control inputs and stability and control derivatives are interpolated using the lookup table. The interpolated trim states and controls are subtracted from the current states and controls to obtain state and control perturbations. The state perturbations $\Delta\mathbf{x} = \mathbf{x} - \mathbf{x}_{trim}\big(\rho(t)\big)$ and control perturbations $\Delta\mathbf{u} = \mathbf{u} - \mathbf{u}_{trim}\big(\rho(t)\big)$ are multiplied by interpolated

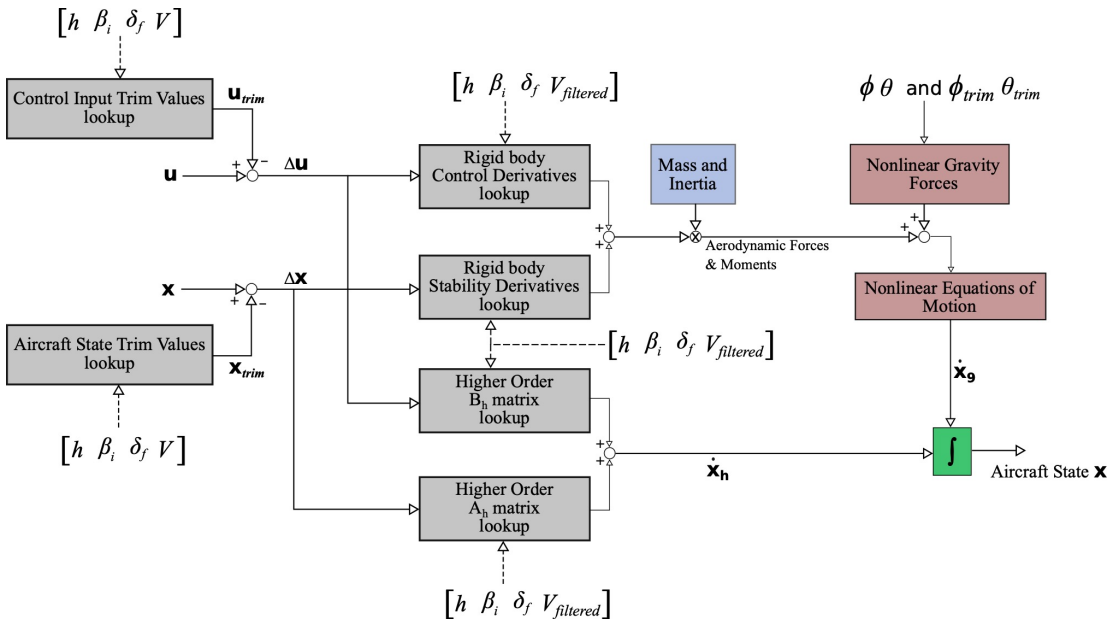

Figure 3: qLPV model structure for XV-15

rigid body stability and control derivatives, respectively and mass matrix to obtain perturbed aerodynamic forces and moments. Also, the state and control perturbations are multiplied by higher order state-space matrices to obtain higher order state derivatives. The interpolation of state-space matrices is based on low-pass filtered velocity $V_{filtered}$ (with a cutoff frequency of $\omega_f = 0.2$ rad/s) to ensure same state derivatives for short term. Nonlinear gravitational forces are added to the perturbed aerodynamic forces and moments and then the nonlinear equations of motion are implemented to obtain rigid body state derivatives. Aircraft states are obtained by integrating the rigid body state derivatives combined with the higher order state derivatives.

Note that the Coriolis terms and linearized gravity terms are removed from state matrix A, as these effects are added in the nonlinear gravitational force equations and nonlinear equations of motion. Moreover, because wing flap angle δ_f is one of the scheduling parameters, control derivatives associated with δ_f in control matrix B are set to zero. The effect of change in δ_f is preserved implicitly in the model by variation in trim states and controls.

2.4 Actuator Dynamics

A first order actuator dynamics model, Eq. 3, is implemented. Time constants and saturation limits (obtained from Marr *et al.* [17]) for each control input are presented in Table 1.

$$G_{act}(s) = \frac{1}{\tau s+1} \tag{3}$$

Actuator Type	Control	Time constant τ [s]	Saturation limit [deg.]	Positive Deflection
Rotor Controls	Collective θ_0	0.040	[-5 49]	Up
	Longitudinal cyclic θ_{1s}		[-10 10]	Forward
	Lateral cyclic θ_{1c}		[-10 10]	Right
Aerodynamic surfaces	Flap δ_f	0.500	[0 75]	Trailing edge down
	Elevator δ_e	0.077	[-20 20]	Trailing edge down
	Aileron δ_a		[-13.8 23.8]	Right trailing edge down
	Rudder δ_r		[-20 20]	Right

Table 1: Actuator time constants and saturation limits

2.5 Time Response Analysis

Figures 4–6 show the Stability and Control Augmentation System (SCAS) OFF response to a longitudinal stick input in helicopter, airplane and conversion mode, respectively. Figures 4 and 5, show the correlation of time histories with NASA's Generic Tilt-Rotor Simulation (GTRS) model [18]. In Figure 6, the correlation is shown with the Flightlab model of XV-15 [19]. In all the figures, qLPV model shows fairly good agreement with GTRS and Flightlab models. The small differences can be explained by the fact that a slightly different gearing ratio for longitudinal stick to elevator K_E is used, when generating the linear state-space models from CAMRAD/JA. $K_E = 4.735$ deg/in. is used, however, in GTRS and Flightlab models $K_E = 4.16$ deg/in is used.

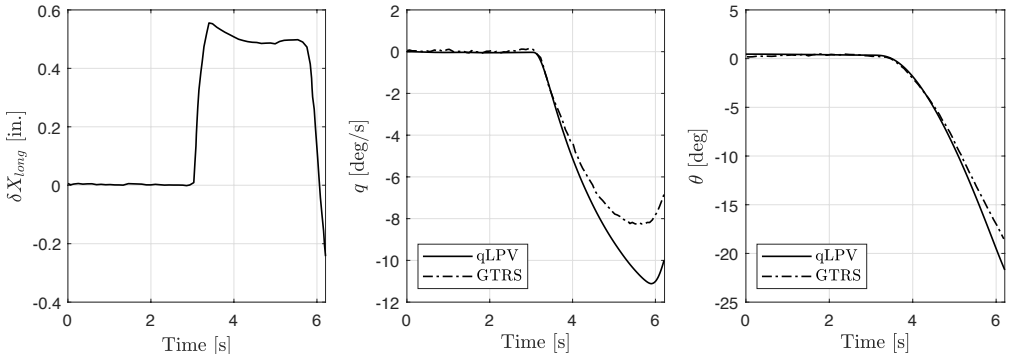

Figure 4: Time history correlation of SCAS OFF pitch response in helicopter mode at 0 kts

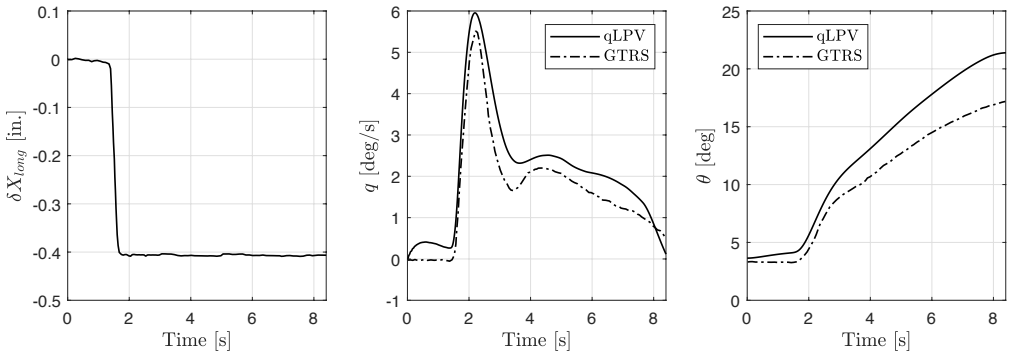

Figure 5: Time history correlation of SCAS OFF pitch response in airplane mode at 175 kts

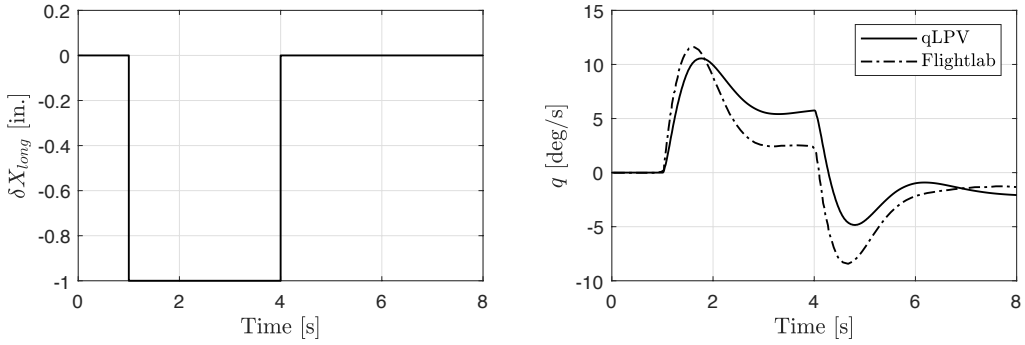

Figure 6: Time history correlation of SCAS OFF pitch response in conversion mode ($\beta_i = 60^0$) at 120 kts

3 LINEAR QUADRATIC TRACKER WITH INTEGRATOR

A gain scheduled linear quadratic tracker with integrator (LQTI) [20] is synthesized for XV-15 to perform the automatic conversion manoeuvre. Block diagram of the LQTI controller for XV-15 is shown in Figure 7.

Consider a state vector $\mathbf{x}(t) = [\mathbf{x}_r(t)\ \ \mathbf{e}_t(t)\ \ \int \mathbf{e}_t(t)\,dt]^T$, where $\mathbf{x}_r(t) \in \Re^n$ is the regulating state vector and $\mathbf{e}_t(t) \in \Re^l$ is the tracking error state vector, then the augmented linear state-space model is given as:

$$\begin{bmatrix}\dot{\mathbf{x}}_r(t)\\ \dot{\mathbf{e}}_t(t)\\ \mathbf{e}_t(t)\end{bmatrix} = \begin{bmatrix}\mathbf{A} & \mathbf{0}\\ \mathbf{A}_{add} & \mathbf{0}\end{bmatrix}\begin{bmatrix}\mathbf{x}_r(t)\\ \boldsymbol{e}_t(t)\\ \int \mathbf{e}_t(t)\,dt\end{bmatrix} + \begin{bmatrix}\mathbf{B}\\ \mathbf{0}\end{bmatrix}\mathbf{u}(t), \qquad \mathbf{A}_{add} = [\mathbf{0} \quad I_{l\times 1}] \tag{4}$$

The performance index to be minimized is:

$$J = \tfrac{1}{2}\int_0^\infty \{x^T(t)Qx(t) + u^T(t)Ru(t)\}\,dt \tag{5}$$

The control input of the LQTI controller that minimizes the performance index is:

$$\begin{aligned}\mathbf{u}(t) &= -K\mathbf{x}(t)\\ K &= [K_r\ \ K_t\ \ K_i]\end{aligned} \tag{6}$$

The control gain consists of regulating gain K_r, tracking gain K_t and integral gain K_i. The LQTI controller is designed for each linear state-space model spanning the conversion corridor and is implemented with qLPV model by scheduling the control gain matrix $K\big(\rho(t)\big)$. In order to ensure global stability of the closed loop qLPV system [21], the control gain matrix is scheduled based on low-pass filtered velocity $V_{filtered}$, similar to **A** and **B** matrices as described in the previous section.

3.1 Automatic Conversion Manoeuvre

An automatic conversion manoeuvre is performed along the centre of conversion corridor at constant reference altitude of 0 ft. The tracking states are velocity and altitude $\mathbf{x}_r = [V\ \ h]$. These states are not part of the linear state-space models and are augmented into the original system by a coordinate transformation using trim pitch angle θ_{trim} and trim angle of attack $\alpha_{trim} = \tan^{-1} {}^{w_{trim}}/_{u_{trim}}$:

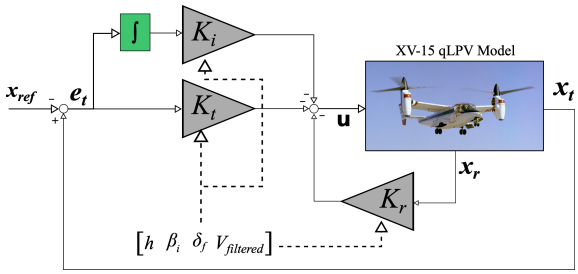

Figure 7: Block diagram of LQTI controller

$$\dot{h}(t) = \mathbf{H}(\rho(t))\mathbf{x}^T(t) = [\sin\theta_{trim}(\rho(t)) \ \ 0 \ \ -\cos\theta_{trim}(\rho(t)) \ \ \mathbf{0}]\mathbf{x}^T(t)$$
$$V(t) = \mathbf{C}(\rho(t))\mathbf{x}^T(t) = [\cos\alpha_{trim}(\rho(t)) \ \ 0 \ \ -\sin\alpha_{trim}(\rho(t)) \ \ \mathbf{0}]\mathbf{x}^T(t) \qquad (7)$$

The linear transformation in above equation is only applied to augment the state matrix in order to design LQTI to track velocity and altitude. Nonlinear $V = \sqrt{u^2 + w^2}$ and $h = u\sin\theta - w\cos\theta$ are used as feedback. The LPV model in Eq. 1, combined with Eq. 4 and Eq. 7, becomes:

$$\begin{bmatrix} \dot{\mathbf{x}}(t) \\ \dot{e}_h \\ \dot{e}_V \\ e_h \\ e_V \end{bmatrix} = \begin{bmatrix} \mathbf{A}(\rho(t)) & 0 & 0 & 0 & 0 \\ \mathbf{H}(\rho(t)) & 0 & 0 & 0 & 0 \\ \mathbf{C}(\rho(t)) & 0 & 0 & 0 & 0 \\ \mathbf{0} & 1 & 0 & 0 & 0 \\ \mathbf{0} & 0 & 1 & 0 & 0 \end{bmatrix} \begin{bmatrix} \mathbf{x}(t) \\ e_h \\ e_V \\ \int e_h\, dt \\ \int e_V\, dt \end{bmatrix} + \begin{bmatrix} \boldsymbol{B}(\rho(t)) \\ 0 \\ 0 \\ 0 \\ 0 \end{bmatrix} \mathbf{u}(t) \qquad (8)$$

For each state-space model in the discrete grid of scheduling parameters $[h \times \delta_f \times \beta_i \times V]$, same state Q and control R weighting matrices are used to compute the control gain matrix K. Diagonal elements of these weighting matrices are presented in Table 2. Conversion manoeuvre is essentially a longitudinal motion and hence very high weights are selected (less contribution) for lateral-directional states and controls. Similarly, as wing flap deflection is one of the scheduling parameters and is not used as input, the weight corresponding to wing flap deflection δ_f is also selected to be very high. Instead, wing flap deflection is scheduled with velocity [22] as shown in Figure 8.

States	Q	Control Inputs	R
u	0.1	θ_{0R}	25000
w	0.1	θ_{1cR}	10^6
q	95000	θ_{1sR}	25000
θ	95000	θ_{0L}	25000
Lateral-Directional states	10^6	θ_{1cR}	10^6
Wing bending and rotor states	20	θ_{1sR}	25000
Wing bending and rotor states derivative	0	δ_f	10^6
e_h	0.5	δ_e	9000
e_V	0.1	δ_a	10^6
$\int e_h\, dt$	2.5	δ_r	10^6
$\int e_V\, dt$	5		

Table 2: Diagonal elements of state and control weighting matrices

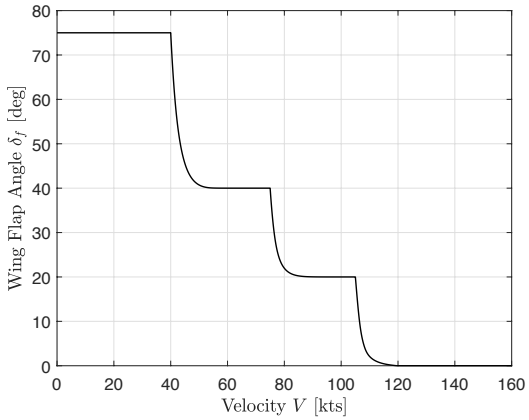

Figure 8: Wing flap deflection with velocity

It should be noted that in XV-15 the gearing ratios from pilot stick inputs to rotor controls are function of nacelle angle, and the rotor controls are progressively phased out as the aircraft converts from helicopter to airplane mode. However, in the current study all control inputs are used throughout the conversion manoeuvre.

The conversion manoeuvre is performed at a constant acceleration $\dot{V} = 4$ kts/s and at a nacelle angle conversion rate $\dot{\beta} = 3$ deg/s for nacelle angles greater than 75° and $\dot{\beta} = 8$ deg/s for nacelle angles less than 75°.

Figure 9 presents the conversion trajectory. Time histories of velocity, nacelle angle and altitude are shown in Figure 10. The performance of LQTI controller is very good in following the reference velocity and keeping the altitude constant. The change in altitude during the complete conversion manoeuvre is within ±10 ft.

Figure 11 presents the evolution of aircraft pitch rate and pitch angle during the conversion manoeuvre. The initial pitch down motion (maximum pitch angle of -20°) is similar to a helicopter pitch down, in order to accelerate from hover to 40 kts. Later, the acceleration is achieved by tilting the nacelle forward.

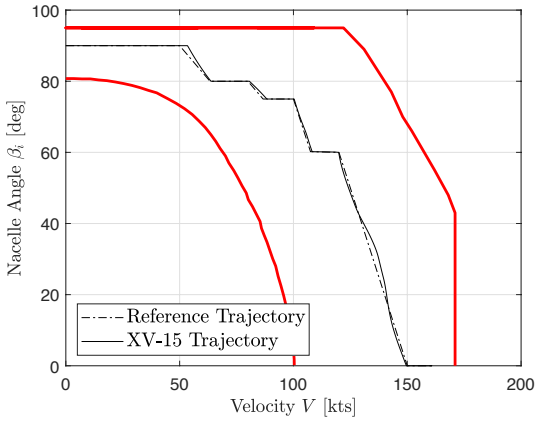

Figure 9: Conversion manoeuvre along the centre of conversion corridor

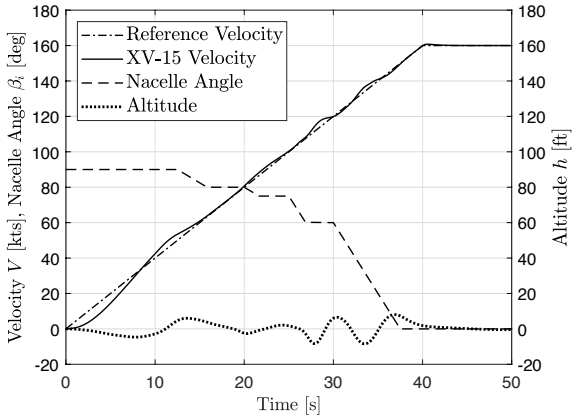

Figure 10: Time histories of velocities, nacelle angle and altitude during centred conversion manoeuvre

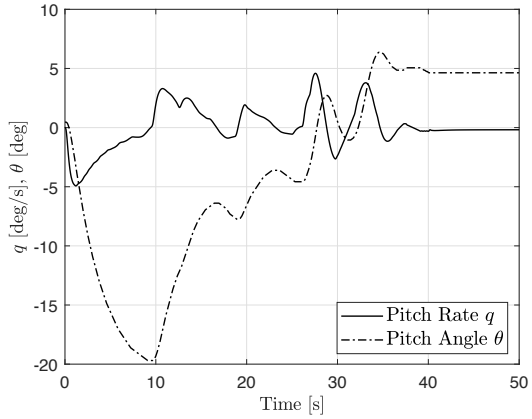

Figure 11: Aircraft pitch rate and pitch angle during centred conversion manoeuvre

Figure 12 shows the variation of control inputs in order to perform centred conversion manoeuvre. As mentioned earlier, no rotor control input is phased out as a function of nacelle angle, rather all the controls are utilized during the conversion manoeuvre. The high demand on longitudinal cyclic θ_{1s} and elevator deflection δ_e (saturation) occurs when nacelle angle starts to tilt from β_i = 60º to 0º.

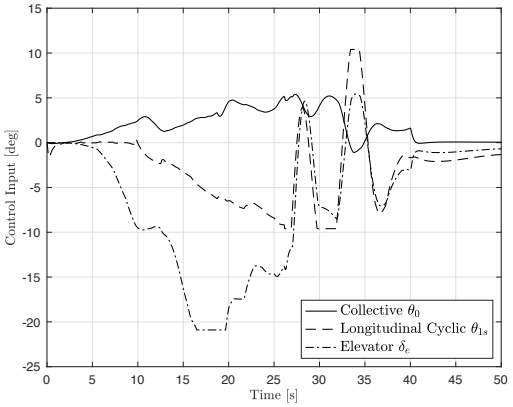

Figure 12: Control inputs to perform centred conversion manoeuvre

Lastly, the longitudinal and lateral gimbal deflections of right rotor are presented in Figure 13. Maximum longitudinal gimbal β_{Gc} corresponds to maximum longitudinal cyclic input, see Figure 12.

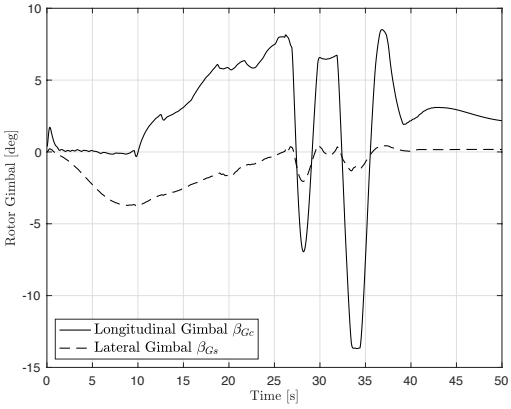

Figure 13: Right rotor gimbal during centred conversion manoeuvre

4 CONCLUSION

In this paper, a high order quasi-Linear Parameter Varying (qLPV) model is developed for XV-15. The qLPV model is scheduled using four-dimensional lookup table: altitude, nacelle angle, wing flap deflection and aircraft velocity. The flight dynamics model is also augmented with actuator dynamics. A gain scheduled linear quadratic tracker with integrator (LQTI) controller is synthesized to perform an automatic conversion manoeuvre.

In the current study, the only control task is to perform conversion manoeuvre i.e., follow a reference velocity while maintaining constant altitude. In the future, other control tasks can be added by utilizing the higher order states. For example, active control for load alleviation during conversion manoeuvre and other handling qualities critical manoeuvres.

Control gain matrix along with the linear state-space models are scheduled using low-pass filtered velocity in order to ensure global stability of qLPV model. However, a robust control approach needs to be developed for qLPV systems to ensure performance and global stability. Further, an effective control allocation technique must be defined in order to utilize the redundant control effectors effectively in all three configurations: helicopter, airplane and conversion mode. Future work will extend to the development of robust nonlinear control synthesis for qLPV systems and effective control allocation techniques for tiltrotor aircraft.

5 ACKNOWLEDGEMENTS

The NITROS (Network for Innovative Training on ROtorcraft Safety) project has received funding from the European Union's Horizon 2020 research and innovation program under the Marie Skłodowska-Curie grant agreement # 721920.

REFERENCES

[1] D. W. King, C. Dabundo, R. L. Kisor, and A. Agnihotri. V-22 Load Limiting Control Law Development. *American Helicopter Society 49th Annual Forum*, St. Loius, Missouri (1993).

[2] B. Manimala, G. D. Padfield, D. Walker, M. Naddei, L. Verde, U. Ciniglio, P. Rollet and F. Sandri. Load Alleviation in Tilt Rotor Aircraft through Active Control; Modelling and Control Concepts. *The Aeronautical Journal*, Vol. **108**, (1082), pp. 169–184 (2004).

[3] M. Maisel. NASA/Army XV-15 Tilt Rotor Research Aircraft Familiarization Document. NASA TM X–62,407 (1975).

[4] D. W. King and P. M. Shultz. Multi-Mode Tiltrotor Nacelle Control System with Integrated Envelope Protection. US Patent No. 6644588 B2 (2003).

[5] J. Kowalski, I. Grill, and R. T. Seminole. Adaptable Automatic Nacelle Conversion for Tilt Rotor Aircraft. US Patent No. 9377784 B2 (2016).

[6] A. Righetti, V. Muscarello and G. Quaranta. Linear Parameter Varying Models for the Optimization of Tiltrotor Conversion Maneuver. *American Helicopter Society 73rd Annual Forum*, Fort Worth, Texas (2017).

[7] A. Marcos and G. J. Balas. Development of Linear-Parameter-Varying Models for Aircraft. *Journal of Guidance, Control and Dynamics*, **Vol. 27**, (2) pp. 218–228 (2004).

[8] E. L. Tobias and M. B. Tischler. A Model Stitching Architecture for Continuous Full Flight-Envelope Simulation for Fixed-Wing Aircraft and Rotorcraft from Discrete-Point Linear Models. U.S. Army AMRDEC SR RDMR–AF–16–01 (2016).

[9] B. Lawrence, C. A. Malpica, and C. R. Theodore. The Development of a Large Civil Tiltrotor Simulation for Hover and Low-speed Handling Qualities Investigations. *36th European Rotorcraft Forum*, Paris, France (2010).

[10] T. Berger, O. Juhasz, M. J. S. Lopez, M. B. Tischler and J. F. Horn. Modeling and Control of Lift Offset Coaxial and Tiltrotor Rotorcraft. *44th European Rotorcraft Forum*, Delft, The Netherlands (2018).

[11] P. Masarati, V. Muscarello, and G. Quaranta. Linearized Aeroservoelastic Analysis of Rotor-Wing Aircraft. *36th European Rotorcraft Forum*, Paris, France (2010).

[12] F. Colombo, V. Muscarello, G. Quaranta and P. Masarati. A Comprehensive Aeroservoelastic Approach to Detect and Prevent Rotorcraft-Pilot Coupling Phenomena in Tiltrotors. *American Helicopter Society 74th Annual Forum*, Pheonix, Arizona (2018).

[13] W. Johnson. CAMRAD/JA, A Comprehensive Analytical Model of Rotorcraft Aerodynamics and Dynamics - Volume I: Theory Manual. Johnson Aeronautics Version (1988).

[14] S. W. Ferguson. A Mathematical Model for Real Time Flight Simulation of a Generic Tilt-Rotor Aircraft. NASA CR 166536 (1988).

[15] C. W. Acree. An Improved CAMRAD Model for Aeroelastic Stability Analysis of the XV-15 with Advanced Technology Blades. NASA TM 4448 (1993).

[16] D. M. Pitt and D. A. Peters. Theoretical Prediction of Dynamic Inflow Derivatives. *6th European Rotorcraft and Powered Lift Aircraft Forum*, Bristol, England, (1980).

[17] R. L. Marr, J. M. Willis and G. B. Churchill. Flight Control System Development for the XV-15 Tilt Rotor Aircraft. *American Helicopter Society 32nd Annual Forum*, Washington, D.C. (1976).

[18] S. W. Ferguson. Development and Validation of a Simulation for a Generic Tilt-Rotor Aircraft. NASA CR 166537 (1989).

[19] G. D. Padfield. "Helicopter Flight Dynamics: Including a Treatment of Tiltrotor Aircraft". John Wiley & Sons, West Sussex, UK, **Vol. 3**, pp. 633 & 670–672 (2018).

[20] J. Jeong, S. Kim, and J. Suk. Control System Design for a Ducted-Fan Unmanned Aerial Vehicle Using Linear Quadratic Tracker. *International Journal of Aerospace Engineering*, **Vol. 2015** (2015).

[21] R. Toth. “Modeling and Identification of Linear Parameter-Varying Systems”. Lecture Notes in Control and Information Sciences, Springer-Verlag Berlin Heidelberg, pp. 93 (2010).

[22] S. Diaz, E. Mouterder and A. Desopper. Performance Code for Take-off and Landing Tilt-Rotor Procedures Study. *30th European Rotorcraft Forum*, Marseilles, France (2004).